Mini review of photoacoustic clinical imaging: a noninvasive tool for disease diagnosis and treatment evaluation

Huazhen Liu, Ming Wang, Fei Ji, Yuxin Jiang, and Meng Yang*
Chinese Academy of Medical Sciences and Peking Union Medical College,
Peking Union Medical College Hospital, Department of Ultrasound, Beijing, China

ABSTRACT. **Significance:** Photoacoustic (PA) imaging is an imaging modality that integrates anatomical, functional, metabolic, and histologic insights. It has been a hot topic of medical research and draws extensive attention.

Aim: This review aims to explore the applications of PA clinical imaging in human diseases, highlighting recent advancements.

Approach: A systemic survey of the literature concerning the clinical utility of PA imaging was conducted, with a particular focus on its application in tumors, auto-immune diseases, inflammatory conditions, and endocrine disorders.

Results: PA imaging is emerging as a valuable tool for human disease investigation. Information provided by PA imaging can be used for diagnosis, grading, and prognosis in multiple types of tumors including breast tumors, ovarian neoplasms, thyroid nodules, and cutaneous malignancies. PA imaging facilitates the monitoring of disease activity in autoimmune and inflammatory diseases such as rheumatoid arthritis, systemic sclerosis, arteritis, and inflammatory bowel disease by capturing dynamic functional alterations. Furthermore, its unique capability of visualizing vascular structure and oxygenation levels aids in assessing diabetes mellitus co-morbidities and thyroid function.

Conclusions: Despite extant challenges, PA imaging offers a promising noninvasive tool for precision disease diagnosis, long-term evaluation, and prognosis antici-pation, making it a potentially significant imaging modality for clinical practice.

1 Introduction

Photoacoustic (PA) imaging is an emerging medical imaging technique that enables detailed visualization of tissue structures and functional information.[1,2] The basis of PA imaging lies in the PA effect, a physical phenomenon in which acoustic waves are generated through light absorption.[1,3,4] The transformation of PA effects from a theoretical concept to a valuable imaging modality has taken over a century of development.[5,6] In recent years, numerous research groups and companies have developed medical devices and processing systems available for human imaging.[1,2,6–8] Typically, PA imaging devices consist of several essential components, including a short-pulsed laser for generating PA signals, an ultrasonic transducer or transducer array for

*Address all correspondence to Meng Yang, amengameng@hotmail.com

detecting PA signals, a data-acquisition system for amplifying and digitizing PA signals, and a computer for forming image.[1,6]

As PA imaging merges laser-induced optical excitation with ultrasound (US) detection, it has advantages for clinical applications as follows: (1) PA imaging allows for noninvasive functional, metabolic, and histological imaging using endogenous contrasts such as hemoglobin [oxygenated hemoglobin (HbO_2), deoxygenated hemoglobin (Hb), total hemoglobin (HbT), also known as total blood volume (TBV)], lipids, and water (Fig. 1);[10–16] (2) PA imaging surpasses the penetration limitations of conventional optical methods, making it superior for deep tissue imaging compared with pure optical imaging techniques;[17] (3) PA imaging can integrate with other imaging modalities, facilitating multimodal approaches that enhance diagnostic accuracy;[18] and (4) PA imaging offers portability in a safe way, making it suitable for longitudinal patient monitoring.[1,19–22] Owing to these advantages, PA imaging has received significant attention in medical research.[7,13,23]

Here, we review promising clinical applications of PA imaging, with a specific focus on tumors, autoimmune diseases, inflammatory conditions, and endocrine disorders. The literature reporting human imaging studies, especially those involving stand-alone multispectral opto-acoustic tomography (MSOT) and hybrid PA and US systems, was primarily reviewed. The aim of this review is to highlight the current advancements in PA imaging. The concluding segment will briefly discuss the challenges that still need to be addressed in PA imaging.

2 Tumor

Malignant tumor is the primary cause of mortality and acts as one of the most important barriers to increasing life expectancy.[24,25] Updated epidemiological data indicate that there were ~19.3 million new cases of cancer and nearly 10.0 million cancer-related deaths worldwide.[25] Hypoxia is a significant hallmark in solid tumors, resulting from the imbalance between the tumor cell proliferation and the available blood supply (Fig. 1).[26,27] This intricate hypoxia micro-environment further leads to the regulation of molecular signaling cascades responsible for fundamental cellular processes, including cell cycle progression and angiogenesis. Tumor-associated hypoxia is related to oncological pathophysiology, including disease progression, therapeutic resistance, and poor outcome.[28–30]

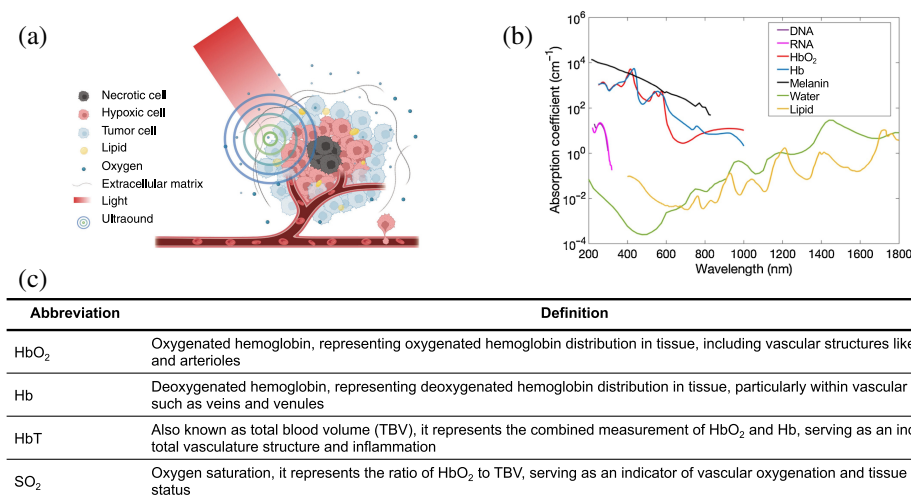| Abbreviation	Definition
HbO_2	Oxygenated hemoglobin, representing oxygenated hemoglobin distribution in tissue, including vascular structures like arteries and arterioles
Hb	Deoxygenated hemoglobin, representing deoxygenated hemoglobin distribution in tissue, particularly within vascular structures such as veins and venules
HbT	Also known as total blood volume (TBV), it represents the combined measurement of HbO_2 and Hb, serving as an indicator of total vasculature structure and inflammation
SO_2	Oxygen saturation, it represents the ratio of HbO_2 to TBV, serving as an indicator of vascular oxygenation and tissue oxygenation status

Fig.1 Schematic diagram of oxygen distribution in solid tumor and PA imaging principles. (a) The peripheral distribution of vasculature in the tumor, revealing decreased oxygen levels in the tumor's center/core, resulting in necrosis. PA imaging involves the absorption of pulsed light by tissue, leading to a rise in temperature and subsequent US wave generation, which is subsequently detected. (b) Absorption spectra of endogenous contrasts. (c) Common terms and definitions used in the detection of hemoglobin in PA imaging. Panel a is created with Ref. 9. Panel b is reprinted with permission from Ref. 10, under the terms of Creative Commons CC BY license.

PA imaging emerges as a compelling paradigm for visualizing the intricate landscape of tumor hypoxia, thereby facilitating early diagnosis and precise evaluation of the tumor.[27,31,32] Its efficacy has been explored in diverse tumors, including breast tumors, ovarian neoplasms, thyroid nodules, and cutaneous malignancies.

2.1 Breast Tumor

Breast tumor is the most common cancer and stands as the primary contributor to cancer-related mortality among women.[25] The overlap in the morphological features between benign and malignant breast tumors poses a great clinical challenge.

PA imaging is a valuable modality for elucidating functional intricacies within breast tumors.[33] In 2011, PA tomography was applied for imaging the vascularity and oxygenation of invasive breast tumors and ductal carcinoma *in situ*.[34] The lesions exhibited an average oxygenation saturation (SO_2) of 78.6%, along with a concentration of HbT measuring 207 μM.[34] Handheld US combined with MSOT also shows the ability for breast tumor imaging.[35–41] MSOT unveiled a pattern of breast cancer characterized by rim enhancement and a diminished core PA signal, evident in both Hb/HbO_2 and TBV images. This pattern correlated with peripheral perfusion but reduced core blood perfusion within the tumor. The findings were validated through postoperative anti-CD31 staining.[35,36]

The precision of breast tumor diagnosis may be improved as PA imaging could provide functional information. The analysis using MSOT revealed significant distinctions in TBV between tumors and normal tissues. Interestingly, disruptions were observed in the water and fat lipid layers in cancerous tissues, potentially suggesting the infiltration of tumors into the adipose tissue.[35] An integrated MSOT/US imaging system exhibited significantly higher hemoglobin signals in invasive carcinoma compared with healthy tissues, indicating increased perfusion in tumor and the tumor environment.[37]

Researchers have also explored various quantitative strategies for characterizing breast tumors. Using a three-dimensional (3D) PA/US functional imaging platform, researchers identified that invasive breast cancer (stage T1) exhibited a 7.7% lower average volumetric SO_2 compared with benign tumors and a 3.9% decrease compared with healthy breast tissue, both statistics significantly. Employing an SO_2 threshold of 78.2%, the model achieved high sensitivity (100%) but moderate specificity (62.5%), resulting in an area under the curve (AUC) of 0.81 for T1 invasive breast cancer differentiation.[39] Further quantitative and semi-quantitative analysis focused on PA signal spatial distribution [Fig. 2(a)].[40] The malignant group displayed significantly greater relative PA signal differences between surrounding/peripheral region and central regions compared with the benign group. A diagnostic model exhibited a strong diagnostic capacity for distinguishing malignancies from benign lesions (sensitivity: 80.8%, specificity: 85.7%, and AUC: 86.5%).[40] Regarding breast intraductal lesions, intraductal lesions exhibited lower SO_2 compared with benign lesions. A diagnostic model, which combined PA-indicated interval vessel data and SO_2 scores, achieved an accuracy rate of 90% sensitivity and 87.5% specificity when discriminating intraductal lesions from benign lesions [Fig. 2(a)].[41] Interestingly, the spatial distribution and spectral analysis of the PA signal may also help distinguish subtypes of breast cancer.[45,46] Luminal breast cancers (both luminal A and luminal B) have exhibited higher external PA signals and lower internal PA signals than those of human epidermal growth factor receptor 2-positive and triple-negative cancers.[45]

The American College of Radiology Breast Imaging Report and Data System (BI-RADS) system is a recognized protocol for diagnosing breast conditions, with its primary emphasis on morphological features of lesions. The incorporation of PA/US enhances the specificity of breast tumor evaluation when compared with grayscale US in isolation.[47] Subsequent investigations endeavored to incorporate the functional data from PA imaging to upgrade and downgrade BI-RADS scores for potentially malignant and benign lesions correspondingly. Benign tumors categorized as BI-RADS 4a could potentially be reclassified to lower categories, thereby decreasing the need for unnecessary biopsies and subsequent follow-up assessments. However, it is important to note that, in a small number of cases, there is a risk of inappropriate reclassification.[48] In the case of intraductal lesions, the PA/US approach led to the upgrading of 40% breast intraductal lesions and the downgrading of 50% benign lesions compared with the BI-RADS system.[41]
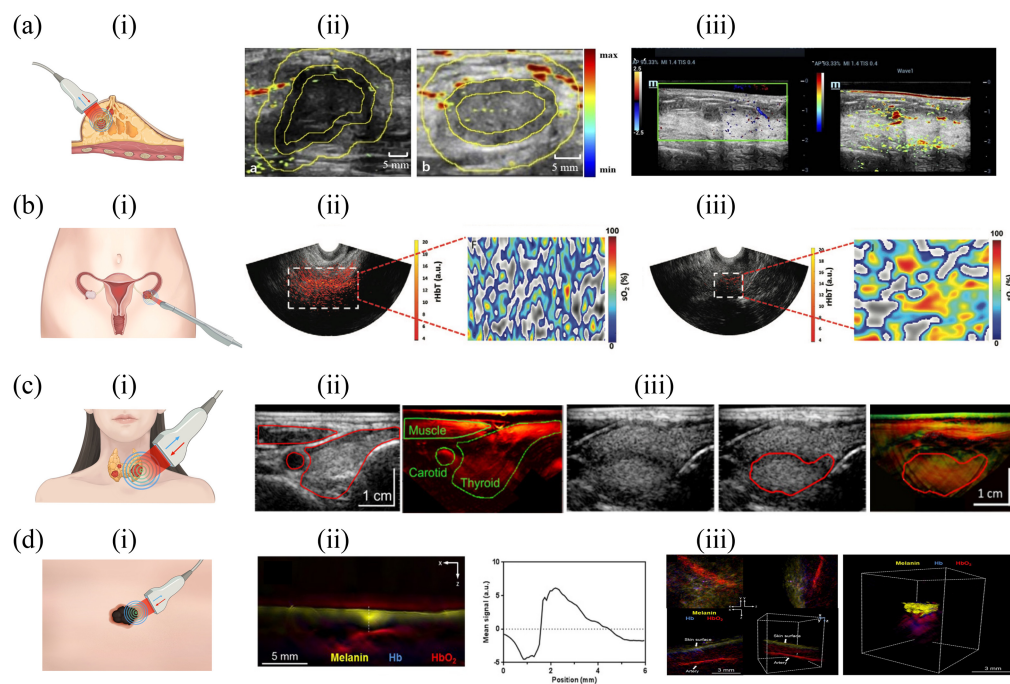
Fig. 2 Representative *in vivo* PA imaging for tumors. (a) Breast tumor PA imaging: (i) a hand-held optoacoustic unit for breast tumor PA imaging. (ii) Left: PA/US modality imaging of a malignant breast lesion (F, 40 years), with limited PA signals in the central region and abundant signals in the peripheral and surrounding regions. Right: PA/US imaging of a benign breast lesion (F, 36 years) with abundant PA signals in all depicted regions. (iii) Intraductal papilloma (F, 65 years). Left: grayscale US with no blood signal indicated by color doppler flow imaging in the lesion. Right: abundant vessel signals indicated by PA. (b) Ovarian tumor PA imaging: (i) A hand-held opto-acoustic unit for ovarian tumor PA imaging. Images of (ii) a 4.5 cm endometrioid adenocarcinoma (F, 63 years) and (iii) a 2.2 cm benign tumor (F, 63y). (ii) A coregistered US/PA image with exten-sive diffused vascular distribution (rHbT map) and an average SO_2 in the region of interest (ROI) of 43.2% (SO_2 map). (iii) The scattered vascular distribution (rHbT map) and an average SO_2 in the ROI of 58.2% (SO_2 map). (c) Thyroid nodule PA imaging: (i) A hand-held optoacoustic unit for thyroid nodule PA imaging. (ii) Thyroid MSOT imaging. Transversal US image (left) and MSOT image (right, showing HbT) of the thyroid gland and surrounding tissue. (iii) MSOT imaging of the benign thyroid nodule. (d) Skin cancer PA imaging: (i) A hand-held optoacoustic unit for skin cancer PA imaging. (ii) MSOT imaging of the superficial basal cell carcinoma acquired by the 2D probe and its distribution along the depth dimension. (iii) Left: 3D MSOT imaging of a viral wart, which identified the large artery by the characteristics of HbO_2 absorption. Right: 3D MSOT imaging of a representative basal cell carcinoma lesion. Melanin signals (yellow) were clus-tered at the top with strong hemoglobin signals underneath the carcinoma (Hb: blue, HbO_2: red). Panel a-ii) is reprinted with permission from Ref. 40 © The Optical Society. Panel a-iii is reprinted with permission from Ref. 41 © The Optical Society. Panels b-ii and b-iii are reprinted with per-mission from Ref. 42 © RSNA. Panels c-ii and c-iii are reprinted with permission from Ref. 43, originally published in JNM, © SNMMI. Panels d-ii and d-iii are reprinted with permission from Ref. 44, under the terms of Creative Commons CC BY license.

2.2 Ovarian Tumor

Ovarian tumors encompass a spectrum of classifications, including benign, borderline, and malignant. Most ovarian malignancies are diagnosed with metastasis, contributing to high gynecological cancer mortality.[49,50] Early differentiation of malignancies from benign/normal masses is important, offering opportunities for prompt multidisciplinary intervention.

Researchers at Washington University School of Medicine employed a transvaginal PA/US system to differentiate ovarian cancer from benign/normal ovaries. Both quantification and spa-tial distribution of hemoglobin contributed significantly. Invasive epithelial cancers exhibited a significantly higher mean relative HbT (rHbT) and displayed an expansive rHbT distribution. By contrast, benign/normal ovaries exhibited scattered distribution. Moreover, the average SO_2 in

invasive epithelial cancers, borderline tumors, and stromal tumors was significantly reduced compared with that in benign or normal ovaries [Fig. 2(b)].[42]

Further enhancement in classification efficacy was achieved through the application of a generalized linear model and support vector machines, increasing AUC from 0.89 to 0.92, and 0.92 to 0.93, respectively.[51] Addressing measurement errors, researchers investigated a multi-pixel method for rHbT and SO_2 estimation. Machine learning models based on support vector machine models trained with significant features achieved an AUC of 0.93 in distinguishing malignant from benign/normal tumors.[52] Moreover, a UNet model, enhanced by US, was developed to improve the accuracy of reconstructing optical absorption distributions within lesions, resulting in an AUC of 0.94.[53]

2.3 Thyroid Nodule

Epidemiological investigations estimate that 4% to 7% of adults have palpable thyroid nodules, with imaging studies identifying nodules up to 10 times more frequently.[54] Although thyroid nodules are relatively common, thyroid cancer is rare, representing ~3% of all malignancies.[25] Clinically, the primary difficulty lies in distinguishing patients with malignant nodules from those with benign nodules. MSOT exhibits the ability to resolve both intranodular microvasculature and extrathyroidal blood vessels, which was verified by histopathology.[55] Researchers use multiparametric PA imaging to classify papillary thyroid carcinoma (PTC) nodules.[56] The PTC nodule had lower SO_2 compared with benign nodules, aligning with the hypothesis of tumor-related hypoxia [Fig. 2(c)].[43,56] A new scoring system in combination with the American Thyroid Association Guideline achieved 83% sensitivity and 93% specificity, potentially reducing unnecessary biopsies in individuals with thyroid nodules.[56]

2.4 Skin Cancer

Skin cancer ranked as the fourth most prevalent new cancer globally.[25] Employing 2D and 3D handheld scanners, MSOT efficiently distinguished tumors and their oxygenation characteristics from normal skin.[44,57,58] Measurements of the tumor dimension through MSOT correlated well with histology findings from excised tumors.[44,59] Real-time 3D imaging could offer insights into the morphology of lesions and the associated neo-vasculature, serving as an indicator of tumor aggressiveness[44] [Fig. 2(d)].

2.5 Surgical Guidance and Therapeutic Efficacy Prediction

PA imaging has been investigated as a method of improving surgical guidance, with a specific focus on improving tumor localization and minimizing damage to non-tumor structures such as nerves and vasculature.[60] This potential application has been explored in a range of tumor types, including pancreatic cancer[61] and pituitary tumors.[62]

Moreover, researchers exploited PA imaging-derived features, notably tumor oxygenation, for predicting treatment responses in cancer patients. Patient-derived xenograft (PDX) models can be used to assess treatment outcomes.[63–67] In the cases of head and neck cancer[64] and triple-negative breast cancer[66] PDX models, the identification of a rise in tumor SO_2 after radiotherapy detected by PA imaging was linked to a notable suppression in tumor growth. The significance of alterations in SO_2 levels as a predictive factor for treatment response has been highlighted in breast cancer cases treated with Bevacizumab[67] and in pancreatic cancer cases responding to suboptimal Cabozantinib.[68] In conclusion, PA imaging may be a straightforward, noninvasive, and cost-effective approach for anticipating therapy efficacy.

3 Autoimmune and Inflammatory Diseases

3.1 Rheumatoid Arthritis, Psoriatic Arthritis, and Osteoarthritis

Rheumatoid arthritis (RA) is a common chronic inflammatory disorder, afflicting around 0.5% to 1% of the general population globally.[69] It is characterized by progressive inflammation of synovial leading to degradation of cartilage, erosion of bone, and subsequent disability.[70] US synovitis scoring provides an accessible, secure, and widely employed tool for assessing and monitoring RA's disease progress.[71] However, gray-scale US might not comprehensively visualize inflamed synovium, and power Doppler US exhibits limitations in detecting

microvessels.[72,73] Consequently, researchers are exploring the utility of PA in detecting subtle inflammatory lesions in RA. Metacarpophalangeal joints of RA patients revealed pronounced hyperemia and hypoxia in inflamed synovium, indicative of heightened metabolic demand and relatively inadequate oxygen supply.[74] Elevated PA signals were detected in RA patients who had evident synovitis, and there was a strong correlation with power Doppler US findings.[75] Zhao et al.[76] developed a semi-quantic PA/US scoring system evaluating seven small joints in RA patients. This PA score exhibited strong positive correlations with key clinical disease activity indices of RA [Fig. 3(a)].[76] Classification of thickened synovium into hyperoxia, intermediate oxygenation status, and hypoxia based on SO_2 values' coloration revealed insightful distinctions. RA patients with hyperoxic synovium displayed a greater abundance of vasculature depicted by Doppler US in comparison with those with hypoxic and intermediate synovium. Individuals with an intermediate oxygen status had lower clinical disease activity indices when compared with those with hypoxia. Notably, the identification of hypoxia within thickened synovium through PA imaging was associated with reduced vascularization and increased disease activity in RA [Fig. 3(a)].[77]

Psoriatic arthritis (PsA) is a heterogeneous inflammatory disorder involving joint, entheses, or skin/nail psoriasis.[79,80] The first step in PsA patent management is the precise and prompt diagnosis that enables timely therapeutic interventions, primarily focusing on the recognition of inflammatory musculoskeletal disease manifestations.[80] Capitalizing on its high sensitivity to inflammation, researchers use MSOT to scrutinize finger joints in PsA patients. The semi-quantitative evaluation of the HbO_2 and Hb PA signals demonstrated that blood content and oxygenation were significantly elevated in PsA patients when compared with individuals from healthy group. This observation underscored the potential of MSOT in the early stage detection of PsA-associated inflammation.[81]
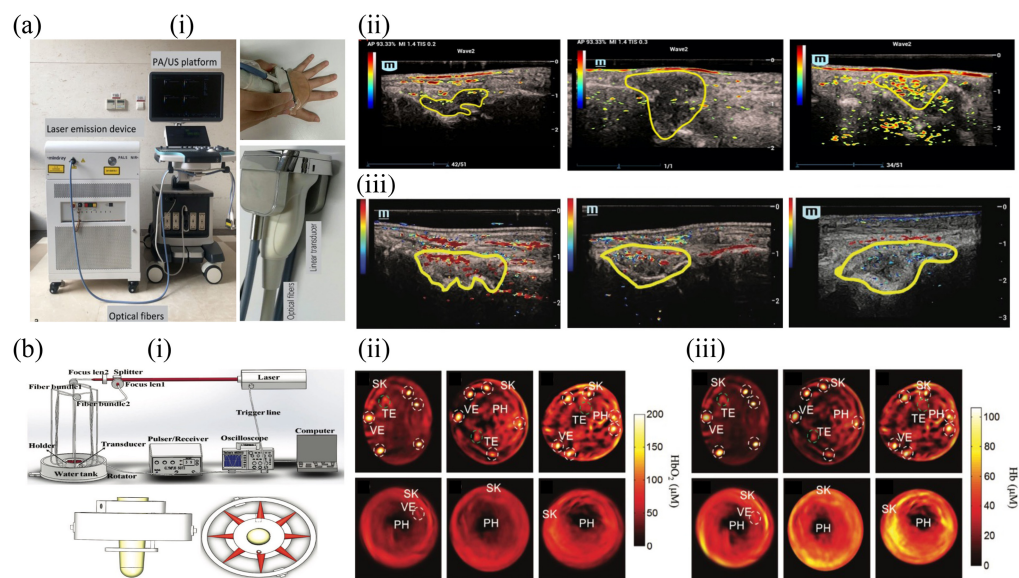

Fig. 3 Representative *in vivo* PA imaging for RA and SSc. (a) PA imaging for RA patients: (i) Photograph of the PA/US system, comprising ultrasonic equipment, a handheld linear PA/US probe, and an optical parametric oscillator tunable laser. (ii) PA examples in the semi-quantic system in thickened synovium: PA 1 (no significant signal, left), PA 2 (PA signals in both the center and margin areas), and PA 3 (abundant PA signals). (iii) SO_2 groupings in thickened synovium, including hyperoxia (left), intermediate status (middle), and hypoxia (right). (b) PA imaging for SSc patients and healthy volunteers: (i) Experimental setup of the PA imaging system and finger holder schematic. (ii) and (iii) The reconstructed HbO_2 and Hb map for healthy volunteers (top) and SSc patients (bottom). TE, tendon; VE, blood vessels; PH, phalanx; SK, skins. Panels a-i and a-ii are reprinted with permission from Ref. 76, under the terms of Creative Commons CC BY license. Panel a-iii is reprinted with permission from Ref. 77 © RSNA. Panel b is reprinted with permission from Ref. 78 © Wiley.

Osteoarthritis (OA) is the most common joint disorder mainly impacting the diarthrodial joints.[82] Evolving from a cartilage-limited perspective, the pathophysiology conception now embraces OA as a multifactorial disease affecting the entirety of the joint structure.[83] In a pilot study, researchers employed multispectral quantitative PA tomography to investigate distal interphalangeal joints of OA patients. Compared with normal joints, OA-affected joints displayed significantly elevated water content, decreased SO_2, and increased acoustic velocity.[84]

3.2 Systemic Sclerosis and Raynaud's Phenomenon

Systemic sclerosis (SSc) is an autoimmune-driven connective tissue disorder identified by microangiopathy and subsequent widespread systemic fibrosis.[85,86] In the early stage of the disease, vascular abnormalities become evident in small blood vessels, and eventually advance to obliterative vasculopathy, leading to issues such as tissue hypoxia, oxidative stress, and vascular complications.[86] Raynaud's phenomenon (RP), marked by pronounced peripheral vasospasm triggered by cold or emotional stress, can lead to severe outcomes including amputation. RP might be primary or secondary, as observed in SSc and other conditions.[87] The inconspicuous alteration in the nail fold microscopic patterns in early SSc patients may find resolution through PA, potentially addressing the clinical imperative for early-stage diagnosis.

Early stage SSc and established SSc patients exhibited significantly diminished SO_2 levels and pronounced skin thickening, distinguishing them from individuals afflicted by primary RP or healthy volunteers [Fig. 3(b)].[78,88,89] Similar results have been obtained using MSOT/US. HbO_2 and HbT of subcutaneous finger tissue measured by MSOT were significantly lower in SSc patients in comparison with those in healthy volunteers.[90] Although the vascular volume remained similar between SSc and healthy control patients, oxygenation within the digital arteries was reduced in SSc patients, indicative of functional impairment. The increase in oxygenation after occlusion release was significantly reduced in individuals with SSc in comparison with the healthy control.[89] Utilizing PA, the differentiation of SSc-RP from healthy volunteers achieved a baseline AUC of 0.72, with elevated diagnosis accuracy observed post-cold stimulus (5 min: AUC = 0.89, 15 min: AUC = 0.91).[91] Furthermore, significantly lower MSOT values in progressive SSc patients compared with those with stable disease were observed, indicating the potential of MSOT to evaluate the disease activity of SSc and monitor therapeutic responses.[90]

3.3 Giant Cell Arteritis

Giant cell arteritis (GCA) is the most common systemic vasculitis in adults.[92] Prominent manifestations include headache, jaw claudication, and visual symptoms, with irreversible vision loss being the most severe complication.[93] Temporal artery biopsy is the gold diagnostic standard for GCA. Noninvasive PA methods are under investigation for early GCA diagnosis. Spectral analysis and the pixel-classification algorithm generated images that closely resembled the findings observed in histopathological examinations. By utilizing minimally supervised spectral analysis, images resembling histology were produced, providing clear delineation between the artery wall and the lumen. Moreover, the PA spectra were successfully distinguished between individuals with biopsy-confirmed GCA and controls.[94]

3.4 Inflammatory Bowel Disease

Idiopathic inflammatory bowel disease is a chronic systemic inflammatory disease predominantly affecting the gastrointestinal tract, encompassing Crohn's disease (CD) and ulcerative colitis (UC).[95] Uncontrolled inflammation is associated with higher complication rates and mortality, which prompts the exploration of novel noninvasive diagnostic and assessment modalities.[96] Researchers used MSOT to evaluate intestinal inflammation in CD patients. US-guided MSOT enabled rapid and noninvasive evaluation of HbT, HbO_2, and Hb content within the intestinal wall. This approach allowed for the quantification of tissue perfusion and oxygenation, which were dependent on hemoglobin and reflected the impact of inflammation.[97] Significant distinctions in measurements at 760 nm and unmixed HbT were observed between remission CD patients identified by endoscopic and active CD patients.[98] In pediatric patients with CD and UC, HbT signals exhibited a significant increase in the terminal ileum of CD patients and in the sigmoid colon of UC patients. There parameters correlated well with the

disease activity, highlighting the potential for noninvasive evaluation in pediatric patients with IBD.[99]

4 Endocrinology and Metabolism Disease

4.1 Diabetes Mellitus

Diabetes mellitus (DM) is a prevalent health issue in the 21st century, presenting a significant public health challenge.[100] DM-related complications include both macrovascular and microvascular conditions, including coronary heart disease, peripheral arterial disease, diabetic kidney disease, and retinopathy.[101]

PA imaging, capable of monitoring perfusion changes,[102] and measuring SO_2 in artery or capillary vessels,[19,103–105] hold promise for staging DM severity via quantitative imaging of vascular complications. Researchers found that, after occlusion, DM patients exhibited a distinctive peripheral hemodynamic response and had lower SO_2 levels than healthy individuals, highlighting the capacity of PA imaging to detect vascular dysfunction of DM (Fig. 4).[106] In addition, MSOT emerged as a tool to visualize peripheral vasculature and assess flow-mediated dilation, which can characterize macrovascular endothelial function—a biomarker for early stage atherosclerosis accentuated in DM.[107] MSOT also displayed potential in imaging peripheral arterial disease, revealing significantly reduced HbO_2, HbT, and SO_2 compared with healthy volunteers.[108] Furthermore, MSOT facilitates the assessment of endocrine and metabolic functions by visualizing lipids and adipose tissue. Reber et al.[109] observed differences in brown adipose tissue composition between DM and healthy volunteers.

Among serious complications associated with DM, poor wound healing, persistent ulceration, and the subsequent need for limb amputation pose significant challenges.[110] Previous studies demonstrated the utility of PA imaging in monitoring wound healing. A case study showed that higher perfusion and SO_2 were correlated with surgical observations. In a cohort, radial artery oxygenation increased significantly after hyperbaric oxygen therapy.[111] Similar outcomes emerged from studies measuring SO_2 following topical hemoglobin treatment, with increased SO_2 predicting treatment response.[112] Moreover, PA imaging can directly visualize angiogenesis.[113] Therapy-responsive patients exhibited evident indications of angiogenesis and a significantly increased rate of PA signals. Negative correlations were detected between the intensity of PA signals and the size of the wound. An increased rate of PA signal or angiogenesis could predict the time of healing within the first 30 days of monitoring.[113]
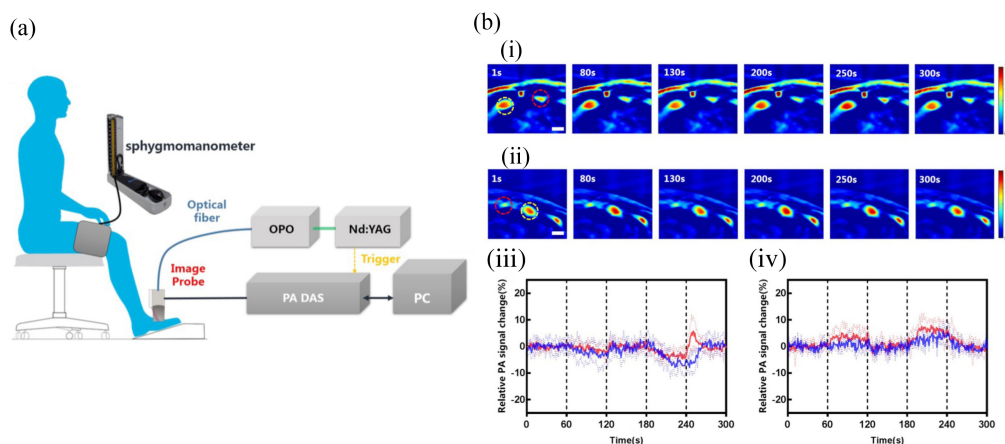

Fig. 4 Representative *in vivo* PA imaging for DM. (a) Schematic of PA tomography system. A sphygmomanometer was used to induce occlusion. PC, personal computer; ND:YAG, laser; OPO, optical parametric oscillator; DAS, data acquisition system. (b) PA imaging during occlusion in healthy and DM patients. (i) and (ii) Sequences of PA images following occlusion in healthy volunteers and DM patients, respectively. (iii) Hemodynamic changes in arteries. (iv) Hemodynamic changes in veins. Blue line: DM; red line: healthy volunteer. Figure 4 is reprinted with permission from Ref. 106 © Wiley.

4.2 Thyroid Disease

The thyroid gland is an important endocrine organ, producing thyroxine to regulate the organ function, metabolic condition, and protein synthesis rate. For imaging of thyroid functional pathology such as Graves' disease (hyperthyroidism) or Hashimoto thyroiditis (hypothyroidism), existing modalities involve assessing the blood flow via Doppler US or tracking the uptake of radioactive contrast agents.[114] PA could reveal microvessels in the human thyroid that escape Doppler US.[115] Further, MSOT could image lipids and water, alongside vascularization and oxygenation predicted on hemoglobin.[19] In Graves' disease patients, HbO_2 and HbT were significantly elevated while fat content exhibited significant reduction, distinguishing them from healthy controls.[43] These initial investigations underscore the capability of PA imaging to offer rapid and radiation-free functional thyroid imaging.[19]

5 Future and Challenges

Over the past decades, PA imaging has demonstrated significant potential in clinical applications, as outlined in this review. The next decade is poised to witness a substantial increase in the utilization of PA imaging in clinical practice, owing to its advantages in penetration depth, functional imaging capabilities, multimodality integration, and safety. However, several challenges remain for the incorporation of PA imaging into routine medical practice.

First, the primary challenge lies in the limited penetration depth.[116] Although PA imaging provides enhanced depth compared with purely optical imaging techniques, inherent attenuation of light energy restricts its penetration to ~3 cm *in vivo* clinical settings.[117,118] Consequently, imaging internal organs such as the heart, liver, pancreas, and uterus in humans remains a challenging task. The exploration of advanced laser technologies and advanced signal processing techniques may help increase the penetration depth. Second, the differentiation of imaging contrast is important. Although endogenous contrasts are various, such as hemoglobin, water, lipid, and melanin, their absorption spectra often overlap, posing difficulties for algorithms to distinguish them, even with MSOT [Fig. 1(b)].[119] This limitation hinders the accuracy of signal quantification and brings uncertainty to PA imaging.[120,121] Investigating contrast agents and employing deep learning algorithms may fascilitate the differentiation of imaging contrasts.[122,123] Third, the absence of standardized protocols is another critical concern. Unlike mature imaging modalities such as MRI and CT, PA imaging lacks standardized procedures and quality control measures.[121,124] This can introduce variability in image quality and interpretation, making it a great challenge to compare results across various studies, institutions, and devices.[7] Establishing education and training procedures for data acquisition and interpretation is imperative. Finally, the deficiency in large-scale clinical validation poses an obstacle. The reliability, accuracy, and value of PA imaging for specific diagnosis and evaluation need to be thoroughly established through well-designed clinical trials.[124]

6 Conclusions

Despite extant challenges, PA imaging exhibits significant promise for both research and clinical applications across diverse fields such as tumors, autoimmune diseases, inflammatory conditions, endocrine disorders, and so on. From bench to bedside, PA imaging aims to facilitate the diagnosis, evaluation, treatment, and prognosis anticipation. Through sustained collaborative efforts among researchers, clinicians, and technologists, PA imaging may pave the way for personalized patient management. As a result, it has the potential to transition from an uncommon technology to a routine strategy, contributing to more precise medical approaches in the foreseeable future.

Disclosures

The authors declare that they have no conflicts of interest.

Code and Data Availability

Data sharing is not applicable to this review, as no new data were created or analyzed.

Acknowledgments

References

1. L. V. Wang and J. Yao, "A practical guide to photoacoustic tomography in the life sciences," *Nat. Methods* **13**(8), 627–638 (2016).
2. W. Choi et al., "Clinical photoacoustic imaging platforms," *Biomed. Eng. Lett.* **8**(2), 139–155 (2018).
3. K. S. Valluru, K. E. Wilson, and J. K. Willmann, "Photoacoustic imaging in oncology: translational pre-clinical and early clinical experience," *Radiology* **280**(2), 332–349 (2016).
4. P. K. Upputuri and M. Pramanik, "Recent advances toward preclinical and clinical translation of photo-acoustic tomography: a review," *J. Biomed. Opt.* **22**(4), 041006 (2017).
5. A. G. Bell, "On the production and reproduction of sound by light," *Am. J. Sci.* **s3-20**(118), 305–324 (1880).
6. J. J. M. Riksen, A.V. Nikolaev, and G. Van Soest, "Photoacoustic imaging on its way toward clinical utility: a tutorial review focusing on practical application in medicine," *J. Biomed. Opt.* **28**(12), 121205 (2023).
7. I. Steinberg et al., "Photoacoustic clinical imaging," *Photoacoustics* **14**, 77–98 (2019).
8. M. Nagli et al., "Silicon photonic acoustic detector (SPADE) using a silicon nitride microring resonator," *Photoacoustics* **32**, 100527 (2023).
9. BioRender.com.
10. T. Zhao et al., "Minimally invasive photoacoustic imaging: current status and future perspectives," *Photoacoustics* **16**, 100146 (2019).
11. S. L. Jacques, "Optical properties of biological tissues: a review," *Phys. Med. Biol.* **58**(11), R37–R61 (2013).
12. V. Ntziachristos and D. Razansky, "Molecular imaging by means of multispectral optoacoustic tomography (MSOT)," *Chem. Rev.* **110**(5), 2783–2794 (2010).
13. M. Taylor-Williams et al., "Noninvasive hemoglobin sensing and imaging: optical tools for disease diagnosis," *J. Biomed. Opt.* **27**(8), 080901 (2022).
14. M. Li, Y. Tang, and J. Yao, "Photoacoustic tomography of blood oxygenation: a mini review," *Photoacoustics* **10**, 65–73 (2018).
15. B. Park et al., "Functional photoacoustic imaging: from nano- and micro- to macro-scale," *Nano Converg.* **10**(1), 29 (2023).
16. S. John et al., "Niche preclinical and clinical applications of photoacoustic imaging with endogenous contrast," *Photoacoustics* **32**, 100533 (2023).
17. L. V. Wang, "Multiscale photoacoustic microscopy and computed tomography," *Nat. Photonics* **3**(9), 503–509 (2009).
18. L. G. Montilla et al., "Real-time photoacoustic and ultrasound imaging: a simple solution for clinical ultra-sound systems with linear arrays," *Phys. Med. Biol.* **58**(1), N1–N12 (2013).
19. A. Karlas et al., "Optoacoustic imaging in endocrinology and metabolism," *Nat. Rev. Endocrinol.* **17**(6), 323–335 (2021).
20. D. Jüstel et al., "Spotlight on nerves: portable multispectral optoacoustic imaging of peripheral nerve vascularization and morphology," *Adv. Sci.* **10**(19), e2301322 (2023).
21. X. L. Deán-Ben and D. Razansky, "Portable spherical array probe for volumetric real-time optoacoustic imaging at centimeter-scale depths," *Opt. Express* **21**(23), 28062–28071 (2013).
22. H. Zhong et al., "Low-cost multi-wavelength photoacoustic imaging based on portable continuous-wave laser diode module," *IEEE Trans. Biomed. Circuits Syst.* **14**(4), 738–745 (2020).
23. S. Zackrisson, S. van de Ven, and S. S. Gambhir, "Light in and sound out: emerging translational strategies for photoacoustic imaging," *Cancer Res.* **74**(4), 979–1004 (2014).
24. F. Bray et al., "Global cancer statistics 2018: GLOBOCAN estimates of incidence and mortality worldwide for 36 cancers in 185 countries," *CA Cancer J. Clin.* **68**(6), 394–424 (2018).
25. H. Sung et al., "Global cancer statistics 2020: GLOBOCAN estimates of incidence and mortality worldwide for 36 cancers in 185 countries," *CA Cancer J. Clin.* **71**(3), 209–249 (2021).
26. D. Nasri et al., "Photoacoustic imaging for investigating tumor hypoxia: a strategic assessment," *Theranostics* **13**(10), 3346–3367 (2023).
27. E. Brown, J. Brunker, and S. E. Bohndiek, "Photoacoustic imaging as a tool to probe the tumour micro-environment," *Dis. Model Mech.* **12**(7), dmm039636 (2019).
28. R. K. Jain, "Normalization of tumor vasculature: an emerging concept in antiangiogenic therapy," *Science* **307**(5706), 58–62 (2005).
29. X. Jing et al., "Role of hypoxia in cancer therapy by regulating the tumor microenvironment," *Mol. Cancer* **18**(1), 157 (2019).

30. T. Dai et al., "Hypoxic activation of PFKFB4 in breast tumor microenvironment shapes metabolic and cellular plasticity to accentuate metastatic competence," *Cell Rep.* **41**(10), 111756 (2022).

31. J. Huang et al., "An activatable near-infrared chromophore for multispectral optoacoustic imaging of tumor hypoxia and for tumor inhibition," *Theranostics* **9**(24), 7313–7324 (2019).

32. L. Lin and L. V. Wang, "The emerging role of photoacoustic imaging in clinical oncology," *Nat. Rev. Clin. Oncol.* **19**(6), 365–384 (2022).

33. S. Manohar and M. Dantuma, "Current and future trends in photoacoustic breast imaging," *Photoacoustics* **16**, 100134 (2019).

34. T. Kitai et al., "Photoacoustic mammography: initial clinical results," *Breast Cancer* **21**(2), 146–153 (2014).

35. G. Diot et al., "Multispectral optoacoustic tomography (MSOT) of human breast cancer," *Clin. Cancer Res.* **23**(22), 6912–6922 (2017).

36. J. Kukačka et al., "Image processing improvements afford second-generation handheld optoacoustic imaging of breast cancer patients," *Photoacoustics* **26**, 100343 (2022).

37. A. Becker et al., "Multispectral optoacoustic tomography of the human breast: characterisation of healthy tissue and malignant lesions using a hybrid ultrasound-optoacoustic approach," *Eur. Radiol.* **28**(2), 602–609 (2018).

38. E. Fakhrejahani et al., "Clinical report on the first prototype of a photoacoustic tomography system with dual illumination for breast cancer imaging," *PLoS One* **10**(10), e0139113 (2015).

39. M. Yang et al., "Quantitative analysis of breast tumours aided by three-dimensional photoacoustic/ultrasound functional imaging," *Sci. Rep.* **10**(1), 8047 (2020).

40. R. Zhang et al., "Exploring the diagnostic value of photoacoustic imaging for breast cancer: the identification of regional photoacoustic signal differences of breast tumors," *Biomed. Opt. Express* **12**(3), 1407–1421 (2021).

41. M. Wang et al., "Functional photoacoustic/ultrasound imaging for the assessment of breast intraductal lesions: preliminary clinical findings," *Biomed. Opt. Express* **12**(3), 1236–1246 (2021).

42. S. Nandy et al., "Evaluation of ovarian cancer: initial application of coregistered photoacoustic tomography and US," *Radiology* **289**(3), 740–747 (2018).

43. W. Roll et al., "Multispectral optoacoustic tomography of benign and malignant thyroid disorders: a pilot study," *J. Nucl. Med.* **60**(10), 1461–1466 (2019).

44. A. B. E. Attia et al., "Noninvasive real-time characterization of non-melanoma skin cancers with handheld optoacoustic probes," *Photoacoustics* **7**, 20–26 (2017).

45. B. E. Dogan et al., "Optoacoustic imaging and gray-scale us features of breast cancers: correlation with molecular subtypes," *Radiology* **292**(3), 564–572 (2019).

46. J. Li et al., "Molecular breast cancer subtype identification using photoacoustic spectral analysis and machine learning at the biomacromolecular level," *Photoacoustics* **30**, 100483 (2023).

47. E. I. Neuschler et al., "A pivotal study of optoacoustic imaging to diagnose benign and malignant breast masses: a new evaluation tool for radiologists," *Radiology* **287**(2), 398–412 (2018).

48. G. L. G. Menezes et al., "Downgrading of breast masses suspicious for cancer by using optoacoustic breast imaging," *Radiology* **288**(2), 355–365 (2018).

49. R. L. Coleman et al., "Latest research and treatment of advanced-stage epithelial ovarian cancer," *Nat. Rev. Clin. Oncol.* **10**(4), 211–224 (2013).

50. S. Lheureux et al., "Epithelial ovarian cancer," *Lancet* **393**(10177), 1240–1253 (2019).

51. E. Amidi et al., "Classification of human ovarian cancer using functional, spectral, and imaging features obtained from *in vivo* photoacoustic imaging," *Biomed. Opt. Express* **10**(5), 2303–2317 (2019).

52. E. Amidi et al., "Role of blood oxygenation saturation in ovarian cancer diagnosis using multi-spectral photoacoustic tomography," *J. Biophotonics* **14**(4), e202000368 (2021).

53. Y. Zou et al., "Ultrasound-enhanced Unet model for quantitative photoacoustic tomography of ovarian lesions," *Photoacoustics* **28**, 100420 (2022).

54. S. B. Fisher and N. D. Perrier, "The incidental thyroid nodule," *CA Cancer J. Clin.* **68**(2), 97–105 (2018).

55. M. E. Noltes et al., "Towards *in vivo* characterization of thyroid nodules suspicious for malignancy using multispectral optoacoustic tomography," *Eur. J. Nucl. Med. Mol. Imaging* **50**(9), 2736–2750 (2023).

56. J. Kim et al., "Multiparametric photoacoustic analysis of human thyroid cancers *in vivo*," *Cancer Res.* **81**(18), 4849–4860 (2021).

57. M. T. Stridh et al., "Photoacoustic imaging of periorbital skin cancer *ex vivo*: unique spectral signatures of malignant melanoma, basal, and squamous cell carcinoma," *Biomed. Opt. Express* **13**(1), 410–425 (2022).

58. T. von Knorring and M. Mogensen, "Photoacoustic tomography for assessment and quantification of cutaneous and metastatic malignant melanoma—a systematic review," *Photodiagn. Photodyn. Ther.* **33**, 102095 (2021).

59. S. Y. Chuah et al., "Structural and functional 3D mapping of skin tumours with non-invasive multispectral optoacoustic tomography," *Skin Res. Technol.* **23**(2), 221–226 (2017).

60. M. S. Karthikesh and X. Yang, "Photoacoustic image-guided interventions," *Exp. Biol. Med.* **245**(4), 330–341 (2020).

61. W. S. Tummers et al., "Intraoperative pancreatic cancer detection using tumor-specific multimodality molecular imaging," *Ann. Surg. Oncol.* **25**(7), 1880–1888 (2018).

62. M. A. Lediju Bell et al., "Localization of transcranial targets for photoacoustic-guided endonasal surgeries," *Photoacoustics* **3**(2), 78–87 (2015).

63. P. Keša et al., "Quantitative *in vivo* monitoring of hypoxia and vascularization of patient-derived murine xenografts of mantle cell lymphoma using photoacoustic and ultrasound imaging," *Ultrasound Med. Biol.* **47**(4), 1099–1107 (2021).

64. L. J. Rich and M. Seshadri, "Photoacoustic monitoring of tumor and normal tissue response to radiation," *Sci. Rep.* **6**, 21237 (2016).

65. L. J. Rich et al., "Photoacoustic imaging as an early biomarker of radio therapeutic efficacy in head and neck cancer," *Theranostics* **8**(8), 2064–2078 (2018).

66. J. Jo et al., "Personalized oncology by *in vivo* chemical imaging: photoacoustic mapping of tumor oxygen predicts radiotherapy efficacy," *ACS Nano* **17**(5), 4396–4403 (2023).

67. I. Quiros-Gonzalez et al., "Photoacoustic tomography detects response and resistance to Bevacizumab in breast cancer mouse models," *Cancer Res.* **82**(8), 1658–1668 (2022).

68. A. Claus et al., "3D ultrasound-guided photoacoustic imaging to monitor the effects of suboptimal tyrosine kinase inhibitor therapy in pancreatic tumors," *Front. Oncol.* **12**, 915319 (2022).

69. J. S. Smolen et al., "Rheumatoid arthritis," *Nat. Rev. Dis. Primers* **4**, 18001 (2018).

70. Q. Guo et al., "Rheumatoid arthritis: pathological mechanisms and modern pharmacologic therapies," *Bone Res.* **6**, 15 (2018).

71. M. A. D'Agostino et al., "Scoring ultrasound synovitis in rheumatoid arthritis: a EULAR-OMERACT ultrasound taskforce-part 1: definition and development of a standardised, consensus-based scoring system," *RMD Open* **3**(1), e000428 (2017).

72. R. Caporali and J. S. Smolen, "Back to the future: forget ultrasound and focus on clinical assessment in rheumatoid arthritis management," *Ann. Rheum. Dis.* **77**(1), 18–20 (2018).

73. H. Nguyen et al., "Prevalence of ultrasound-detected residual synovitis and risk of relapse and structural progression in rheumatoid arthritis patients in clinical remission: a systematic review and meta-analysis," *Rheumatology* **53**(11), 2110–2118 (2014).

74. J. Jo et al., "A functional study of human inflammatory arthritis using photoacoustic imaging," *Sci. Rep.* **7**(1), 15026 (2017).

75. P. J. van den Berg et al., "Feasibility of photoacoustic/ultrasound imaging of synovitis in finger joints using a point-of-care system," *Photoacoustics* **8**, 8–14 (2017).

76. C. Zhao et al., "Multimodal photoacoustic/ultrasonic imaging system: a promising imaging method for the evaluation of disease activity in rheumatoid arthritis," *Eur. Radiol.* **31**(5), 3542–3552 (2021).

77. M. Yang et al., "Synovial oxygenation at photoacoustic imaging to assess rheumatoid arthritis disease activity," *Radiology* **306**(1), 220–228 (2023).

78. Y. Liu et al., "Imaging molecular signatures for clinical detection of scleroderma in the hand by multispectral photoacoustic elastic tomography," *J. Biophotonics* **11**(6), e201700267 (2018).

79. D. J. Veale and U. Fearon, "The pathogenesis of psoriatic arthritis," *Lancet* **391**(10136), 2273–2284 (2018).

80. O. FitzGerald et al., "Psoriatic arthritis," *Nat. Rev. Dis. Primers* **7**(1), 59 (2021).

81. S. Hallasch et al., "Multispectral optoacoustic tomography might be a helpful tool for noninvasive early diagnosis of psoriatic arthritis," *Photoacoustics* **21**, 100225 (2021).

82. S. Glyn-Jones et al., "Osteoarthritis," *Lancet* **386**(9991), 376–387 (2015).

83. J. Martel-Pelletier et al., "Osteoarthritis," *Nat. Rev. Dis. Primers* **2**, 16072 (2016).

84. J. Xiao and J. He, "Multispectral quantitative photoacoustic imaging of osteoarthritis in finger joints," *Appl. Opt.* **49**(30), 5721–5727 (2010).

85. C. P. Denton and D. Khanna, "Systemic sclerosis," *Lancet* **390**(10103), 1685–1699 (2017).

86. E. R. Volkmann, K. Andréasson, and V. Smith, "Systemic sclerosis," *Lancet* **401**(10373), 304–318 (2023).

87. F. M. Wigley and N. A. Flavahan, "Raynaud's phenomenon," *N. Engl. J. Med.* **375**(6), 556–565 (2016).

88. K. Daoudi et al., "Photoacoustic and high-frequency ultrasound imaging of systemic sclerosis patients," *Arthritis Res. Ther.* **23**(1), 22 (2021).

89. S. Wilkinson et al., "Photoacoustic imaging is a novel tool to measure finger artery structure and oxygenation in patients with SSc," *Sci. Rep.* **12**(1), 20446 (2022).

90. M. Masthoff et al., "Multispectral optoacoustic tomography of systemic sclerosis," *J. Biophotonics* **11**(11), e201800155 (2018).

91. J. R. Eisenbrey et al., "Photoacoustic oxygenation quantification in patients with Raynaud's: first-in-human results," *Ultrasound Med. Biol.* **44**(10), 2081–2088 (2018).

92. D. Pugh et al., "Large-vessel vasculitis," *Nat. Rev. Dis. Primers* **7**(1), 93 (2022).

93. F. Buttgereit, E. L. Matteson, and C. Dejaco, "Polymyalgia rheumatica and giant cell arteritis," *JAMA* **324**(10), 993–994 (2020).

94. M. Naumovska et al., "Mapping the architecture of the temporal artery with photoacoustic imaging for diagnosing giant cell arteritis," *Photoacoustics* **27**, 100384 (2022).
95. C. Abraham and J. H. Cho, "Inflammatory bowel disease," *N. Engl. J. Med.* **361**(21), 2066–2078 (2009).
96. G. G. Kaplan and J. W. Windsor, "The four epidemiological stages in the global evolution of inflammatory bowel disease," *Nat. Rev. Gastroenterol. Hepatol.* **18**(1), 56–66 (2021).
97. M. J. Waldner et al., "Multispectral optoacoustic tomography in Crohn's disease: noninvasive imaging of disease activity," *Gastroenterology* **151**(2), 238–240 (2016).
98. F. Knieling et al., "Multispectral optoacoustic tomography for assessment of Crohn's disease activity," *N. Engl. J. Med.* **376**(13), 1292–1294 (2017).
99. A. P. Regensburger et al., "Multispectral optoacoustic tomography enables assessment of disease activity in paediatric inflammatory bowel disease," *Photoacoustics* **35**, 100578 (2024).
100. D. Tomic, J. E. Shaw, and D. J. Magliano, "The burden and risks of emerging complications of diabetes mellitus," *Nat. Rev. Endocrinol.* **18**(9), 525–539 (2022).
101. J. M. Forbes and M. E. Cooper, "Mechanisms of diabetic complications," *Physiol. Rev.* **93**(1), 137–188 (2013).
102. Y. Mantri et al., "Monitoring peripheral hemodynamic response to changes in blood pressure via photoacoustic imaging," *Photoacoustics* **26**, 100345 (2022).
103. C. P. Favazza, L. A. Cornelius, and L. V. Wang, "*In vivo* functional photoacoustic microscopy of cutaneous microvasculature in human skin," *J. Biomed. Opt.* **16**(2), 026004 (2011).
104. J. Bunke et al., "Photoacoustic imaging for the monitoring of local changes in oxygen saturation following an adrenaline injection in human forearm skin," *Biomed. Opt. Express* **12**(7), 4084–4096 (2021).
105. C. Lee et al., "Panoramic volumetric clinical handheld photoacoustic and ultrasound imaging," *Photoacoustics* **31**, 100512 (2023).
106. J. Yang et al., "Detecting hemodynamic changes in the foot vessels of diabetic patients by photoacoustic tomography," *J. Biophotonics* **13**(8), e202000011 (2020).
107. A. Karlas et al., "Flow-mediated dilatation test using optoacoustic imaging: a proof-of-concept," *Biomed. Opt. Express* **8**(7), 3395–3403 (2017).
108. A. Karlas et al., "Multispectral optoacoustic tomography of peripheral arterial disease based on muscle hemoglobin gradients—a pilot clinical study," *Ann. Transl. Med.* **9**(1), 36 (2021).
109. J. Reber et al., "Non-invasive measurement of brown fat metabolism based on optoacoustic imaging of hemoglobin gradients," *Cell Metab.* **27**(3), 689–701.e4 (2018).
110. U. A. Okonkwo and L. A. DiPietro, "Diabetes and wound angiogenesis," *Int. J. Mol. Sci.* **18**(7), 1419 (2017).
111. Y. Mantri et al., "Photoacoustic imaging to monitor outcomes during hyperbaric oxygen therapy: validation in a small cohort and case study in a bilateral chronic ischemic wound," *Biomed. Opt. Express* **13**(11), 5683–5694 (2022).
112. M. Petri et al., "Oxygenation status in chronic leg ulcer after topical hemoglobin application may act as a surrogate marker to find the best treatment strategy and to avoid ineffective conservative long-term therapy," *Mol. Imaging Biol.* **20**(1), 124–130 (2018).
113. Y. Mantri et al., "Photoacoustic monitoring of angiogenesis predicts response to therapy in healing wounds," *Wound Repair Regen.* **30**(2), 258–267 (2022).
114. J. P. Walsh, "Managing thyroid disease in general practice," *Med. J. Aust.* **205**(4), 179–184 (2016).
115. M. Yang et al., "Photoacoustic/ultrasound dual imaging of human thyroid cancers: an initial clinical study," *Biomed. Opt. Express* **8**(7), 3449–3457 (2017).
116. L. V. Wang and S. Hu, "Photoacoustic tomography: *in vivo* imaging from organelles to organs," *Science* **335**(6075), 1458–1462 (2012).
117. K. S. Valluru and J. K. Willmann, "Clinical photoacoustic imaging of cancer," *Ultrasonography* **35**(4), 267–280 (2016).
118. B. Cox et al., "Quantitative spectroscopic photoacoustic imaging: a review," *J. Biomed. Opt.* **17**(6), 061202 (2012).
119. J. Yao and L. V. Wang, "Photoacoustic microscopy," *Laser Photonics Rev.* **7**(5), 758–778 (2013).
120. M. Sivaramakrishnan et al., "Limitations of quantitative photoacoustic measurements of blood oxygenation in small vessels," *Phys. Med. Biol.* **52**(5), 1349–1361 (2007).
121. J. Joseph et al., "Evaluation of precision in optoacoustic tomography for preclinical imaging in living subjects," *J. Nucl. Med.* **58**(5), 807–814 (2017).
122. H. Deng et al., "Deep learning in photoacoustic imaging: a review," *J. Biomed. Opt.* **26**(4), 040901 (2021).
123. C. Yang et al., "Review of deep learning for photoacoustic imaging," *Photoacoustics* **21**, 100215 (2021).
124. H. Assi et al., "A review of a strategic roadmapping exercise to advance clinical translation of photoacoustic imaging: from current barriers to future adoption," *Photoacoustics* **32**, 100539 (2023).

Huazhen Liu received her MD from Peking Union Medical College (PUMC). She is a postdoctoral researcher in the Department of Ultrasound, PUMC Hospital. Her research

interests focus on the clinical applications of photoacoustic imaging, with a particular emphasis on rheumatoid arthritis and oncology.

Ming Wang received her MD from PUMC Hospital in 2014. She was an attending physician in the Department of Ultrasound, PUMC Hospital, where she participated in research on breast imaging and musculoskeletal imaging. Since 2017, she has been involved in clinical studies on photoacoustic/ultrasound functional imaging, with a specific focus on its clinical application for breast cancer.

Fei Ji is a resident in ultrasonography at PUMC Hospital, China. Her research interests pertain to gynecological disease, musculoskeletal disease, and multimodal photoacoustic/ultrasonic imaging system.

Yuxin Jiang is a professor in the Department of Ultrasound Medicine, PUMC Hospital. He holds the China branch chairman position at the International Society of Ultrasound in Obstetrics and Gynecology (ISUOG) and serves as the vice chairman of the Asian Federation for Societies of Ultrasound in Medicine and Biology (AFSUMB). His professional interests include breast cancer, thyroid and parathyroid diseases, kidney disorders, and the application of contrast-enhanced ultrasonography in liver and thyroid diseases.

Meng Yang received her MD from PUMC, Beijing, China and pursued postdoctoral research at the Molecular Imaging Program at Stanford University (MIPS). Currently, she serves as a chief physician at PUMC Hospital. Her interests span the development of photoacoustic/ultrasound (PA/US) imaging systems and the clinical translation of PA/US imaging in thyroid, breast, dermatologic, musculoskeletal, and obstetrics and gynecology diseases.